# FINAL REPORT FOR MOISTURE EFFECTS ON COMPACTION OF FIBERBOARD IN A 9975 SHIPPING PACKAGE

T. M. Stefek
W. L. Daugherty
E. G. Estochen

Savannah River National Laboratory
Materials Science & Technology

Publication Date: March 2013

**Savannah River Nuclear Solutions**
**Savannah River Site**
**Aiken, SC 29808**

This document was prepared in conjunction with work accomplished under Contract No. DE-AC09-08SR22470 with the U.S. Department of Energy.

**Final Report for Moisture Effects on Compaction of Fiberboard in a 9975 Shipping Package**

APPROVALS:

T. M. Stefek ____________________ Date ____________________
Author, Materials Science and Technology

W. L. Daugherty ____________________ Date ____________________
Author, Materials Science and Technology

E. G. Estochen ____________________ Date ____________________
Author, Materials Science and Technology

L. C. Olson ____________________ Date ____________________
Technical Reviewer, Materials Science and Technology

K. A. Dunn ____________________ Date ____________________
Pu Surveillance Program Lead, Materials Science and Technology

G. T. Chandler ____________________ Date ____________________
Manager, Materials App & Process Tech

E. R. Hackney ____________________ Date ____________________
NMM Engineering

REVIEWS:

D. R. Leduc ____________________ Date ____________________
Savannah River Packaging Technology

## Revision Log

**Document No.** SRNL-STI-2012-00347 **Rev. No.** 0

**Document Title** **Final Report for Moisture Effects on Compaction of Fiberboard in a 9975 Shipping Package**

| Rev. # | Page # | Description of Revision | Date |
|---|---|---|---|
| 0 | all | Original document | 9/17/2013 |

## SUMMARY

Compaction of lower layers in the fiberboard assembly has been observed in 9975 packages that contain elevated moisture. Lab testing has resulted in a better understanding of the relationship between the fiberboard moisture level and compaction of the lower fiberboard assembly, and the behavior of the fiberboard during transport. In laboratory tests of cane fiberboard, higher moisture content has been shown to correspond to higher total compaction, greater rate of compaction, and continued compaction over a longer period of time. In addition, laboratory tests have shown that the application of a dynamic load results in higher fiberboard compaction compared to a static load.

The test conditions and sample geometric/loading configurations were chosen to simulate the regulatory requirements for 9975 package input dynamic loading. Dynamic testing was conducted to acquire immediate and cumulative changes in geometric data for various moisture levels. Two sample sets have undergone a complete dynamic test regimen, one set for 27 weeks, and the second set for 47 weeks. The dynamic input, data acquisition, test effects on sample dynamic parameters, and results from this test program are summarized and compared to regulatory specifications for dynamic loading.

Compaction of the bottom fiberboard layers due to the accumulation of moisture is one possible cause of an increase in the axial gap at the top of the package. The net compaction of the bottom layers will directly add to the axial gap. The moisture which caused this compaction migrated from the middle region of the fiberboard assembly (which is typically the hottest). This will cause the middle region to shrink axially, which will also contribute directly to the axial gap. Measurement of the axial gap provides a screening tool for identifying significant change in the fiberboard condition. The data in this report provide a basis to evaluate the impact of moisture and fiberboard compaction on 9975 package performance during storage at the Savannah River Site (SRS).

## BACKGROUND

This is a final report of Task 1 tests carried out per Task Technical and Quality Assurance Plan SRNS-TR-2010-00044, "TTQAP for Testing of Moisture Effects on Model 9975 Package" [1], which is part of the comprehensive 9975 package surveillance program [2]. Task 1 tests were developed to determine the impact of fiberboard moisture level on compaction under load.

Experience with fiberboard compaction includes the identification of several packages in which the axial gap has increased and exceeded the response threshold of 1 inch. This observation was generally accompanied by elevated moisture levels in the bottom fiberboard layers and compaction of those layers [3, 4]. Elevated moisture might accumulate within the fiberboard due to the introduction of moisture to the package, or by the concentration of existing moisture into local regions through migration under thermal gradient. The impact of elevated moisture on fiberboard properties and the response of the package to changing moisture conditions have been described [5]. Over time, elevated moisture levels will accelerate the degradation of thermal, mechanical and physical fiberboard properties [6, 7].

## EXPERIMENTAL APPROACH

Laboratory tests have been performed to compare material properties and/or the response of fiberboard to transient loadings for different time scales using four test methods as listed in Table 1.

- Short-term tests measured the fiberboard response under load within a single, very long load cycle.
- Standard compression tests subjected the samples to a single half-cycle loading event.
- Dynamic tests have subjected the samples to a dynamic load of varying frequency and amplitude, such as might occur during handling and transport.
- Damping tests determined fiberboard damping level dependence on moisture and applied load.

Table 1. Test Matrix

| Sample ID | TargetTest Conditions | | Actual Test Conditions | | | |
|---|---|---|---|---|---|---|
| | Stress (psi) | % WME | Weight (lbs) | Sample Length (inches) | Sample Width (inches) | Calculated Actual Stress (psi) |
| **Short-Term Tests** | | | | | | |
| S1 | 3.4 / 6.8 | 10 | 50 / 100 | 3.903 | 3.905 | 3.3 / 6.6 |
| S2 | 2.7 / 5.4 | 20 | 40 / 80 | 3.861 | 3.865 | 2.7 / 5.4 |
| S3 | 2.7 / 5.4 | 30 | 40 / 80 | 3.846 | 3.882 | 2.7 / 5.4 |
| S4 | 3.4 / 6.8 | 15 | 50 / 100 | 3.913 | 3.911 | 3.3 / 6.5 |
| S5 | 2.7 / 5.4 | 25 | 40 / 80 | 3.847 | 3.856 | 2.7 / 5.4 |
| S6 | 2.7 / 5.4 | 35 | 40 / 80 | 3.856 | 3.812 | 2.7 / 5.4 |
| S10 | 2.7 / 5.4 | 10 | 40 / 80 | 3.899 | 3.915 | 2.6 / 5.2 |
| S15 | 2.7 / 5.4 | 15 | 40 / 80 | 3.914 | 3.930 | 2.6 / 5.2 |
| S15B | 2.7 / 5.4 | 15 | 40 / 80 | 3.937 | 3.876 | 2.6 / 5.2 |
| S25 | 2.7 / 5.4 | 25 | 40 / 80 | 3.928 | 3.946 | 2.6 / 5.2 |
| S30 | 2.7 / 5.4 | 30 | 40 / 80 | 3.845 | 3.822 | 2.7 / 5.4 |
| S30B | 2.7 / 5.4 | 30 | 40 / 80 | 3.905 | 3.905 | 2.6 / 5.2 |
| S35 | 2.7 / 5.4 | 35 | 40 / 80 | 3.912 | 3.892 | 2.6 / 5.3 |
| S40 | 2.7 / 5.4 | 29.4 wt% | 40 / 80 | 3.919 | 3.890 | 2.6 / 5.2 |
| S50 | 2.7 / 5.4 | 32.0 wt% | 40 / 80 | 3.888 | 3.883 | 2.6 / 5.3 |
| S40B | 2.7 / 5.4 | 40.0 wt% | 40 / 80 | 3.852 | 3.860 | 2.7 / 5.4 |
| S47 | 2.7 / 5.4 | 46.9 wt% | 40 / 80 | 3.852 | 3.856 | 2.7 / 5.4 |
| **Compression Tests** | | | | | | |
| LD2 | n/a | 7.5 - 12.5 | n/a | 2" nom | 2" nom | 0 to >6000 |
| New | n/a | 6.7 - 12.0 | n/a | 2" nom | 2" nom | 0 to >6000 |
| 02028 | n/a | 10.9 | n/a | 2" nom | 2" nom | 0 to >6000 |

| Sample ID | TargetTest Conditions | | Actual Test Conditions | | | |
|---|---|---|---|---|---|---|
| | Stress (psi) | % WME | Weight (lbs) | Sample Length (inches) | Sample Width (inches) | Calculated Actual Stress (psi) |
| **Dynamic Tests** | | | | | | |
| 50C | 3.4 | 10 | 50 | 3.923 | 3.909 | 3.3 |
| 40E | 2.7 | 20 | 40 | 3.825 | 3.846 | 2.7 |
| 40F | 2.7 | 30 | 40 | 3.821 | 3.837 | 2.7 |
| D-50-6 | 3.4 | 6 | 50 | 3.854 | 3.860 | 3.4 |
| D-40-25 | 2.7 | 25 | 40 | 3.84 | 3.872 | 2.7 |
| D-40-35 | 2.7 | 35 | 40 | 3.861 | 3.857 | 2.7 |
| **Dynamic Tests (control samples)** | | | | | | |
| 50A | 3.4 | 10 | 50 | 3.910 | 3.911 | 3.3 |
| 40A | 2.7 | 20 | 40 | 3.848 | 3.856 | 2.7 |
| 40C | 2.7 | 30 | 40 | 3.861 | 3.866 | 2.7 |
| S-50-6 | 3.4 | 6 | 50 | 3.872 | 3.867 | 3.3 |
| S-50-10 | 3.4 | 10-15 | 50 | 3.859 | 3.860 | 3.4 |
| S-40-25 | 2.7 | 25 | 40 | 3.876 | 3.877 | 2.7 |
| S-40-35 | 2.7 | 35 | 40 | 3.869 | 3.876 | 2.7 |
| **Damping Tests** | | | | | | |
| H-10 | 0.7 - 3.4 | 10 | 10, 22, 32, 40, 50 | 3.934 | 3.882 | 0.7 - 3.3 |
| H-20 | 0.7 - 3.4 | 20 | 10, 22, 32, 40, 50 | 3.875 | 3.922 | 0.7 - 3.3 |
| H-30 | 0.7 - 3.4 | 30 | 10, 22, 32, 40, 50 | 3.943 | 3.940 | 0.6 - 3.2 |
| D-40-25 | 0.7 - 3.4 | 10 | 10, 32, 50 | 3.875 | 3.922 | 0.7 - 3.3 |
| D-40-35 | 0.7 - 3.4 | 20 | 10, 32, 50 | 3.943 | 3.940 | 0.6 - 3.2 |
| D-50-6 | 0.7 - 3.4 | 20 | 10, 32, 50 | 3.934 | 3.882 | 0.7 - 3.3 |

The moisture level of each sample was varied by either drying the sample in an oven, or conditioning the sample in a high humidity environment until the desired moisture level was reached. The moisture level in each sample was confirmed using a GE Protimeter Surveymaster moisture meter for samples up to saturation (28 wt %). The moisture level in samples above saturation was confirmed by comparing conditioned sample weight to dry sample weight, since the moisture meter response is non-linear above saturation.

While the short-term and compression tests offer a simpler look at the basic response of the fiberboard under a single dynamic cycle, the dynamic tests better simulate the conditions a package might experience in service. Preliminary results for each test method were presented in a paper at the Institute for Nuclear Materials Management (INMM) Annual Meeting in 2010 [8].

The lead shield (and the containment vessels and payload contained within) sits on an aluminum bearing plate embedded within the lower fiberboard assembly (Figure 1). The bearing plate, shield, containment vessels and a typical loaded 3013 container place a load of approximately 263 pounds on the fiberboard.

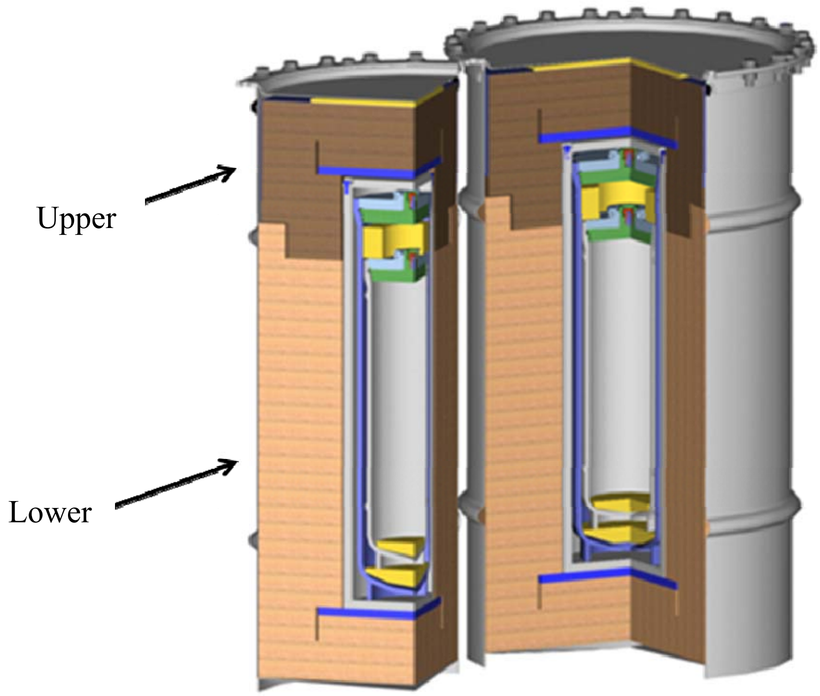


Figure 1. Cross section of the 9975 shipping package showing the configuration of the fiberboard overpack. The upper and lower fiberboard assemblies are indicated (arrows).

The bottom of the 9975 outer drum is dished (Figure 2), and the fiberboard overpack is fabricated with a flat bottom. Typically, a ring of compressed fiberboard will form around the outer edge of the bottom surface approximately 1½ - 2 inches wide. As the bottom layer(s) compress further (due to increased loading or reduced fiberboard strength), this ring will widen until the entire fiberboard bottom surface is in contact with the drum bottom. This has been observed in packages with elevated moisture content, and is illustrated in Figure 2. With the limited contact area, the peak stress in the bottom fiberboard layers is typically no greater than 3.4 psi. As the compressed region widens, the peak stress decreases to 2.7 psi, which is the stress immediately under the bearing plate.

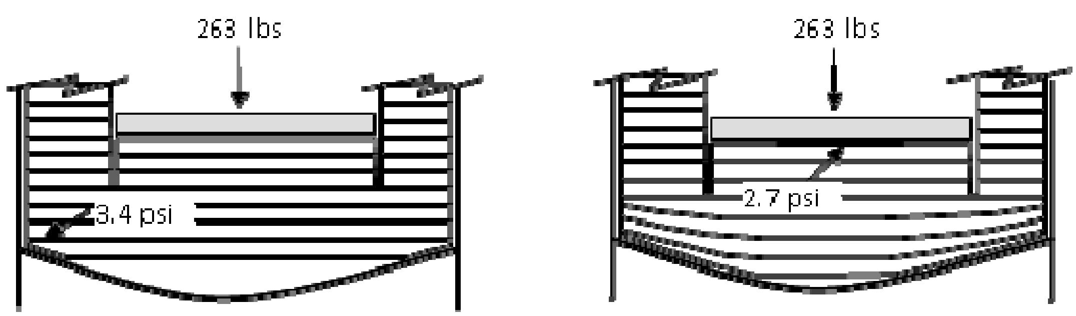


Figure 2. Varying degree of contact between the lower fiberboard assembly and drum bottom. As the contact area increases, the peak fiberboard stress will decrease to that immediately under the bearing plate. NOTE: Degree of curvature exaggerated for visual effect.

**Short-Term Testing**

Samples approximately 4 x 4 x 2 inches in size were removed from a single cane fiberboard assembly (Package 9975-02028). This package was removed from service in K-Area and testing showed the fiberboard to be non-degraded compared to new fiberboard. Each sample is maintained at a specific moisture content. Each sample is sealed within a plastic bag to help maintain a constant moisture level throughout testing. Short-term testing was conducted in two stages. In the first stage, the sample moisture level ranges from approximately 10 to 35 %WME (wood moisture equivalent)[1] and two sample stress levels are used. For nominal moisture samples (10 - 15 %WME), the target stress is approximately 3.4 psi. For higher moisture content (20 - 35 %WME), the target stress is approximately 2.7 psi. In the second stage, the sample moisture level ranges from approximately 10 %WME to above saturation (up to approximately 47 wt %) and a target stress of 2.7 psi is used for all samples. In the first stage, the dual stress levels approximate the varying maximum stresses actually experienced in a package. In the second stage, the single stress level provides a better basis for extrapolating fiberboard behavior to other conditions.

The sample stress is achieved by placing a weight on each sample (see Figure 3). The initial load is placed on each sample (loaded perpendicular to the fiberboard layers), and the sample height allowed to stabilize. The degree of compression is measured repeatedly until it appears stable (typically up to several days). This represents the equilibrium static condition for the bottom fiberboard layers within a 9975 package. The load on each sample is then doubled (to 5.4 or 6.8 psi) as a static equivalent cycle of dynamic loading. The doubled load is then reduced to the prior level as the material rebound is measured.

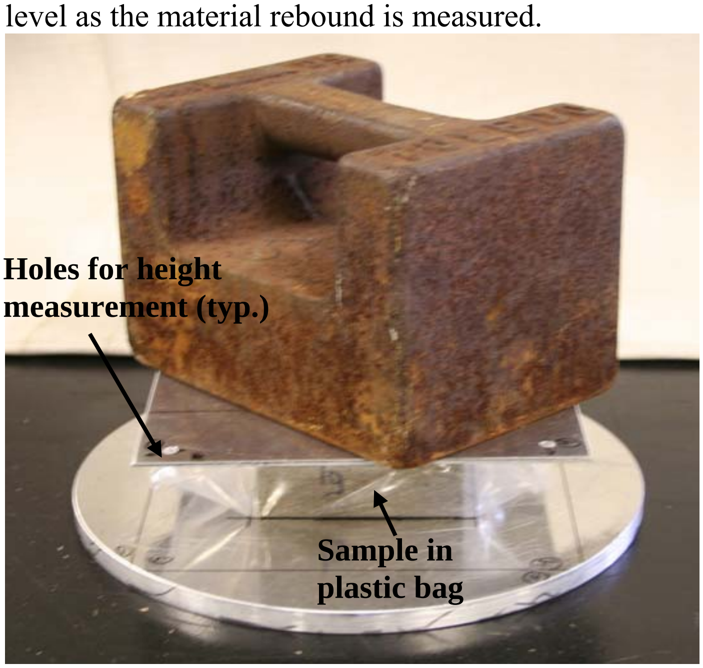


Figure 3. Typical test setup for short-term test sample. Sample height is measured in-situ by extending calipers through each of 4 holes in the upper plate.

[1] %WME represents the electrical resistivity measured by a wood moisture meter. For cane fiberboard, it relates to moisture content by: wt% moisture ≅ 0.67 * %WME + 2.6, over a range of 6 to ~40 %WME.

The height of each sample is measured by extending a caliper through each of 4 holes in the plate on top of the sample. By averaging these 4 measurements, variation from tipping if the sample compresses non-uniformly is eliminated. The thickness of the plate is subtracted from the measurement to get the actual sample height. In the short-term tests, the initial loading cycle is indicative of the response of the lower layers of the fiberboard assembly when the package is first assembled. Similarly, the second loading cycle approximates the response during some period of handling or transport, and removal of the higher load represents an end to the dynamic activity as the package sits in storage.

**Compression Testing**

A set of 8 compression samples (~2 x 2 x 2 inch) were tested using an Instron Mechanical Tensile Tester with the load applied perpendicular to the fiberboard layers, and using a crosshead speed of 1.9 inch/minute. The samples were taken from several different non-degraded package assemblies which were tested previously [5, 6]. Package-to-package variability was observed, and data from two packages (LD2 and New) which bounded the compression test data, are included in this report. These two packages had moisture content ranging from 6.7 to 12.5 %WME (~7 to 11 wt%), which is similar to the seasonal variation for material in equilibrium with the ambient humidity [9]. A ninth compression sample was taken from the same package as the short-term and dynamic test samples (Package 9975-02028). This sample was tested at a moisture content of 10.9 %WME to provide direct comparison to results from the other test methods, while avoiding package-to-package variation.

The compression test behavior of fiberboard has been described previously [7, 10]. While a compression test typically extends to high strain levels, the data of current interest includes low compressive strain behavior corresponding to stress levels of < 10 psi.

**Dynamic Testing**

Samples approximately 4 x 4 x 2 inches in size were removed from the same fiberboard assembly used for short-term tests (Package 9975-02028). Two sets of samples were prepared for testing. The first set included three samples that contain moisture levels of approximately 10, 20 and 30 %WME. The second set included three samples that contain moisture levels of approximately 6, 25, and 35 %WME. Both sets included duplicate static samples which were not subjected to dynamic loading. Each sample was enclosed within a box or bag to help maintain a constant moisture level throughout testing. The target stress for nominal moisture samples (6 - 15 %WME) was approximately 3.4 psi. For higher moisture content ($\geq$ 20 %WME), the target stress was approximately 2.7 psi. These compressive stresses were achieved by placing a weight on each sample.

Vibration from road transportation loadings identified in the 9975 SARP [11] is bounded by a high amplitude low frequency envelope of 1 – 1.5 g at 2 – 7 Hz, and a power spectral density value of 0.001 $g^2$/Hz in the frequency range from 10-40 Hz. The samples were placed on a cart, and the dynamic loadings resulted as the cart was moved over a rough surface (metal plates mounted to an expanded metal sheet) according to a set pattern (see Figure 4). The transport cycle simulation was performed weekly, and consisted of pushing the cart down the test surface and pulling it back nine times. This cycle was completed in 90 seconds. On one occasion (first set, at 7 weeks), the transport cycle simulation was extended to include 90 trips down the test surface and back over a duration of 900 seconds. Sample height and moisture content were recorded weekly. Sample height was measured through the top plate in 4 locations, as described previously in the short-term testing section. For the dynamic samples, the degree of sample compression was measured before and after each transport cycle simulation.

Figure 4. Test setup of the dynamic load test for samples
(A) Sample boxes on cart (B) Arrangement within sample boxes

The cart wheels are 5 inches in diameter and are made of plastic with a solid rubber tire. The dynamic load, transmitted to the samples by rolling the cart over the rough surface, was recorded using accelerometers. One accelerometer (PCB model #353B33, Sensitivity=0.104 Volt/g) was screw mounted to the top of the sample enclosure, and a second accelerometer (Kistler model #8630B5, Sensitivity=0.984 Volt/g) was mounted with wax adhesive to the floor of the cart proximate to a corner.

**Damping Testing**

During dynamic compaction experiments, it was observed that fiberboard damping levels were related to moisture level and/or compressive loading. Several experiments were formulated to determine damping dependence on moisture and applied load. The damping dependence experiments were conducted to use the following parametric variations to identify the effects of changes in moisture and applied load:

a. For a given fiberboard moisture, compressive load was varied from 10 to 50 pounds (10 pound increments), and damping measured.
  - Objective: Determine the fiberboard damping as a function of compressive load.

b. The experiment in “a.” was repeated for moisture levels of 10 to 50 %WME (~10% increments).
  - Objective: Determine fiberboard damping as a function of moisture.

c. Two additional samples were tested with a 40 pound compressive load, one with ~10 %WME, and one with ~20 %WME, and damping measured. Samples remained under 40 pound static compressive load, and damping measured weekly until damping showed negligible change.

- Objective: Determine if time dependent creep or fiberboard sag affects damping.

Damping experiments used fiberboard rectangular samples approximately 4” x 4”x 2”. These samples were removed from Package 9975-02028 fiberboard assembly. An impulse-response type modal test was performed, where an instrumented hammer (load cell between tip and head) is used to impact an item while measuring item response with an accelerometer. Data acquisition using a Fast Fourier Transform (FFT) analyzer facilitates conversion of data from the time domain to the frequency domain, where Transfer Function measurements indicate the presence of system resonant frequencies when the ratio of acceleration response to force input is plotted as a function of frequency. Figure 5 shows a depiction of the experimental set-up used to acquire the Transfer Functions, from which data required for damping determination were extracted. Specific technical details related to data acquisition, signal processing and data reduction are documented in a separate reference along with the raw data obtained from the experiments [12].

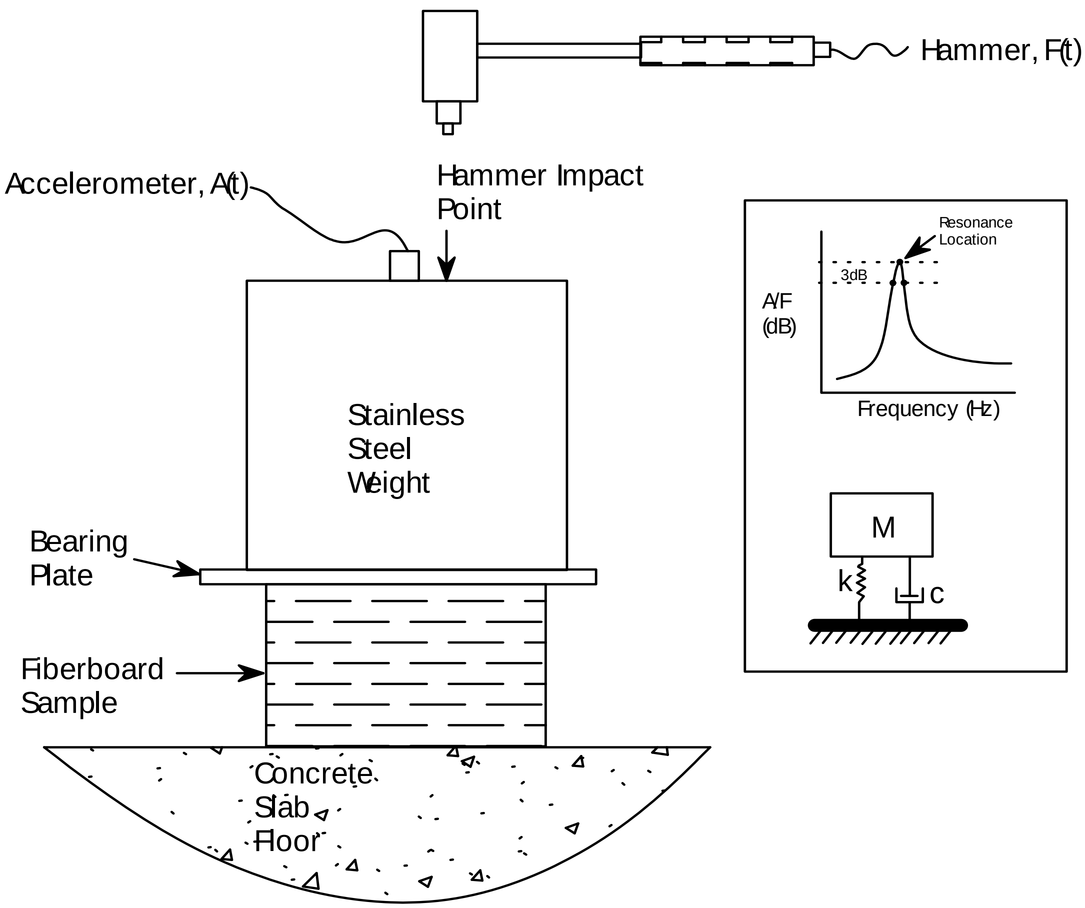


Figure 5. Damping experimental set-up

## RESULTS

### Short-Term Testing

The short-term samples were maintained under load for varying periods, depending on the sample response. The change in sample height during loading and unloading for first stage samples is shown in Figure 6A. The change in height during loading and unloading for second stage samples is shown in Figure 6B.

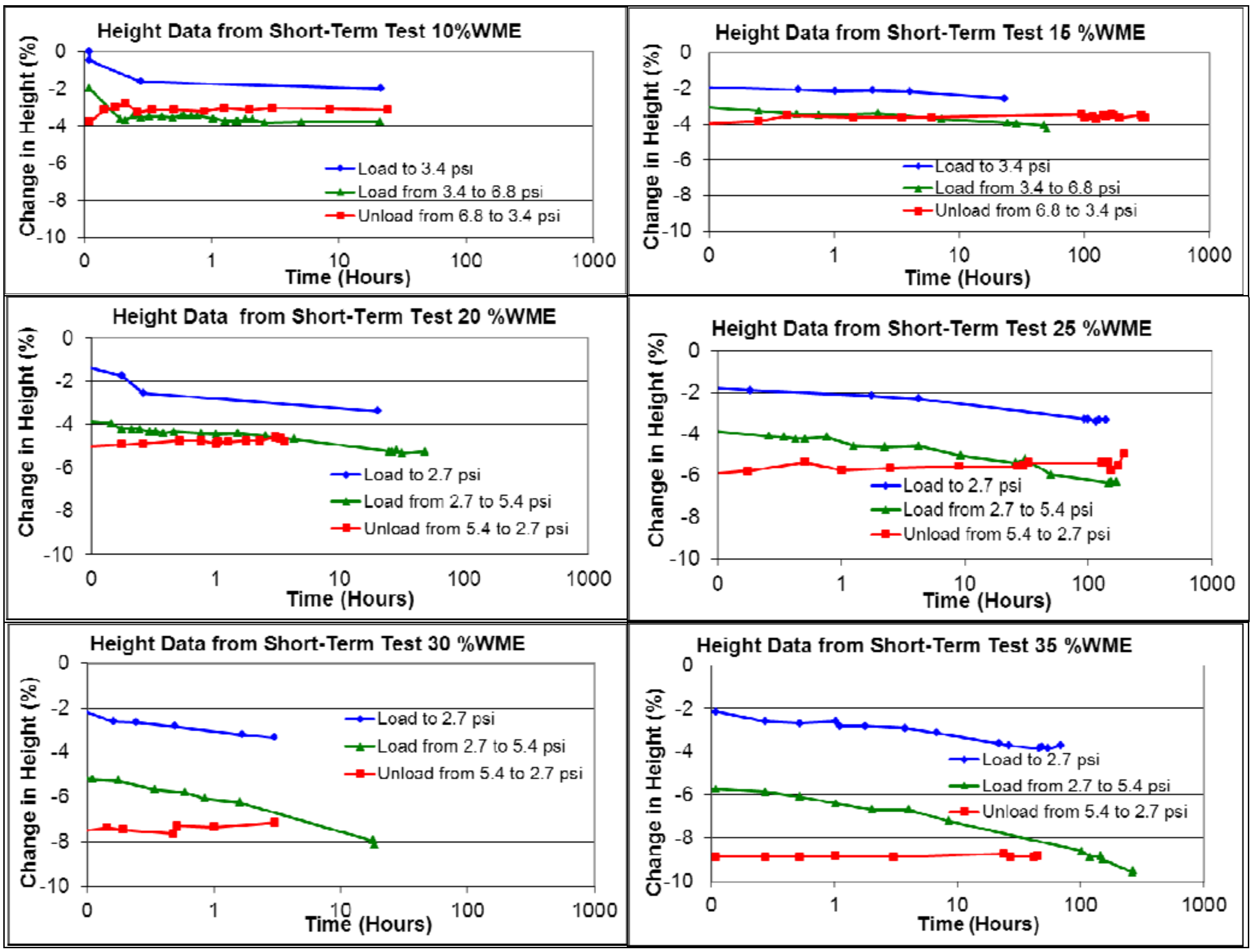


Figure 6A. Change in sample height during short-term testing for first stage samples

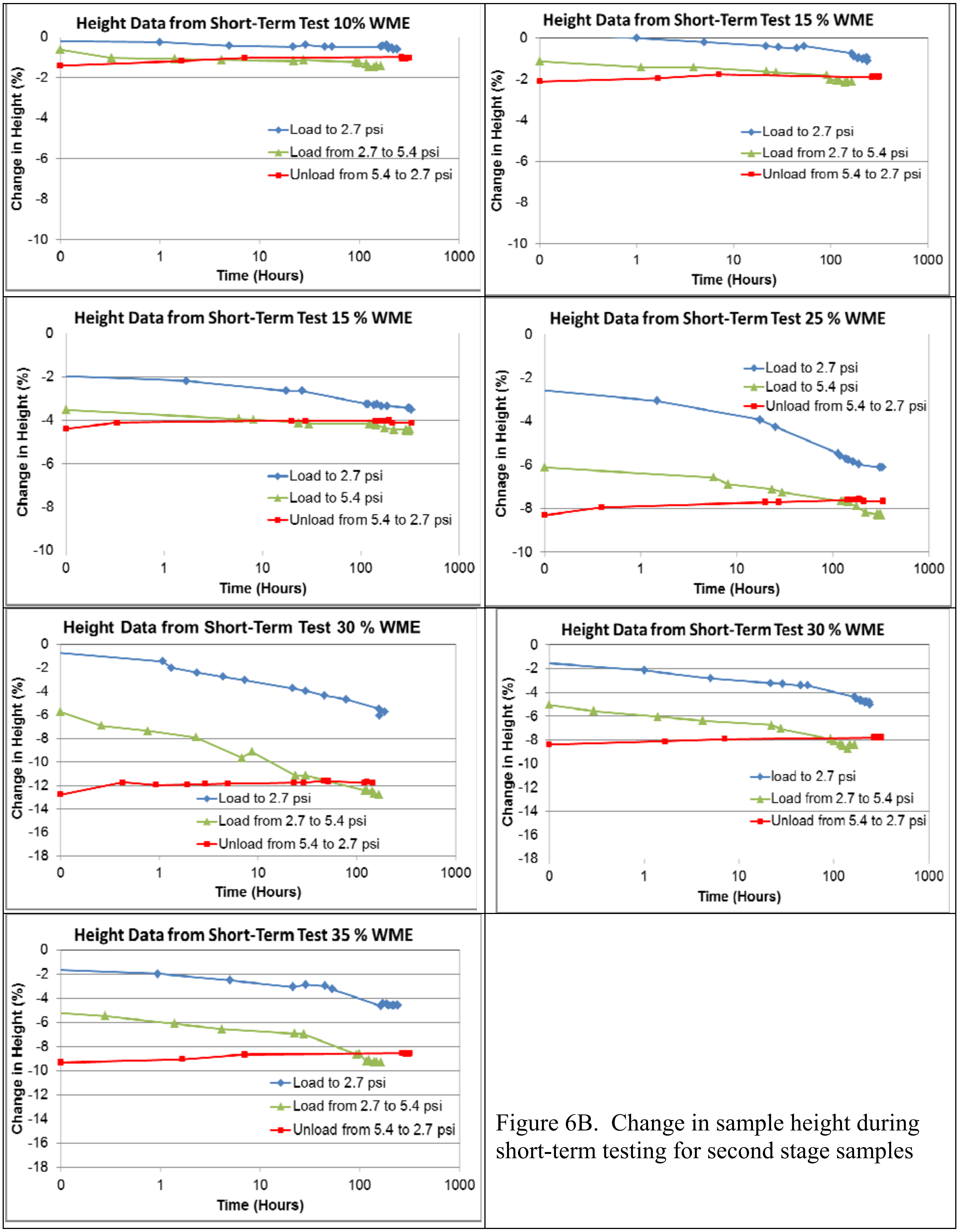


Figure 6B. Change in sample height during short-term testing for second stage samples

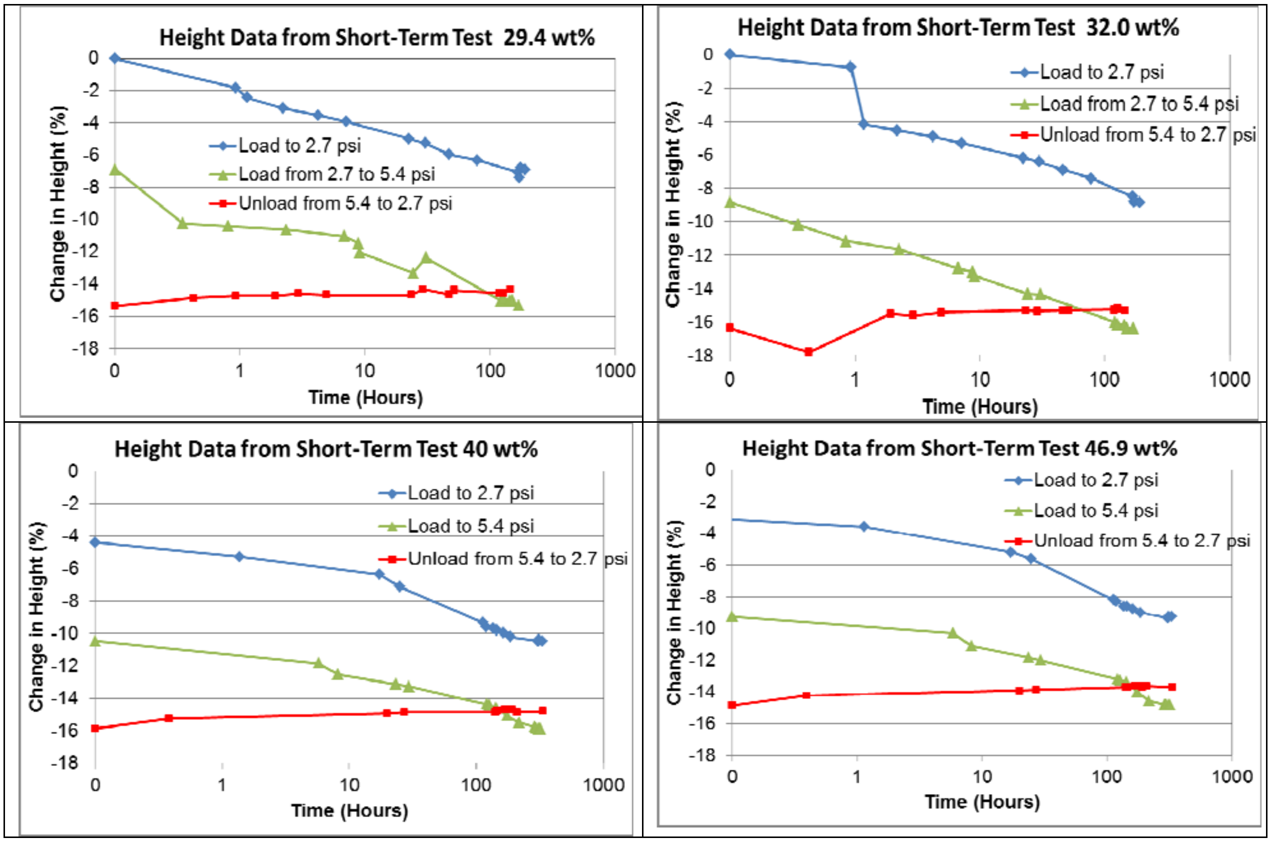

Figure 6B (continued). Change in sample height during short-term testing for second stage samples

## Compression Testing

A range of fiberboard stress-strain response is seen based on package-to-package variation in addition to variation from moisture content (Figure 7A). The area of interest in the compression test curve is at very low stress (~3 – 5 psi). However, the stress-strain curve is not always consistent in this range due to minor sample misalignment, machine slack, etc. Therefore, this behavior is approximated by the slope of the stress-strain curve at a slightly higher stress (~10 - 20 psi) and extrapolating to lower values. This is illustrated in Figure 7B for source package LD2. The slope for each sample is summarized in Table 2 along with the extrapolated degree of compression at stresses of 3.4 and 6.8 psi.

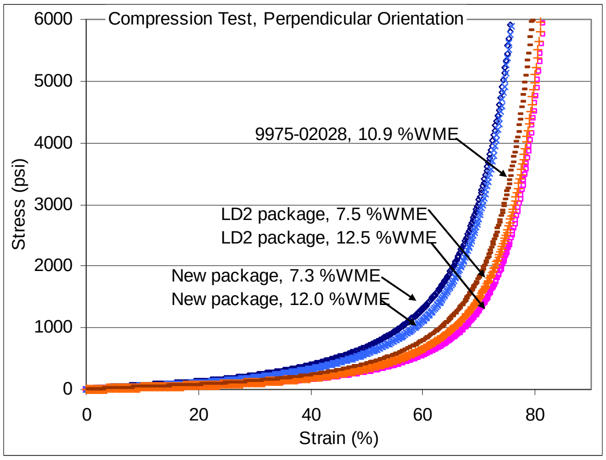


Figure 7A. Stress strain curves for fiberboard from two packages at two moisture levels, compared to package 9975-02028.

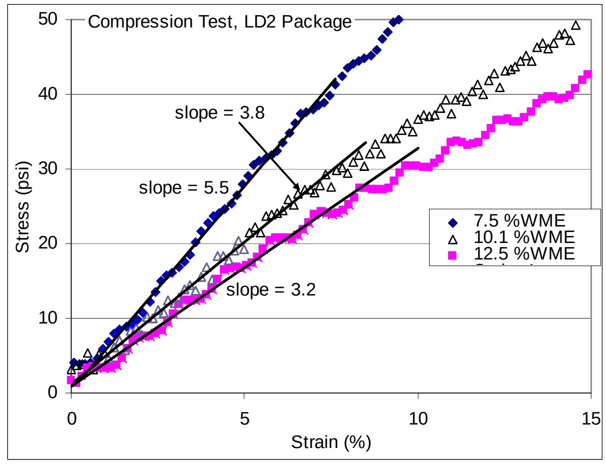


Figure 7B. Low stress portion of compression test curves for LD2 package samples, with slope fit to lower section of the curve.

Table 2. Summary of slopes from low stress portion of compression test curves, with extrapolated estimates of compression (percentage loss of original height) at select stress levels.

| **Package LD2** | **Package New** | **9975-02028** |
|---|---|---|
| **Slope of compression curve @ moisture level** | | |
| | 7.5 psi/% @ 6.7 %WME | |
| 5.5 psi/% @ 7.5 %WME | 8.7 psi/% @ 7.3 %WME | |
| 3.8 psi/% @ 10.1 %WME | | 4.9 psi/% @10.9 WME |
| 3.2 psi/% @ 12.5 %WME | 7.5 psi/% @ 12.0 %WME | |
| | | |
| **Estimated sample compression at 3.4 psi** | | |
| 0.62% @ 7.5 %WME | 0.39% @ 7.3 %WME | |
| | | 0.69% @10.9 %WME |
| 1.06% @ 12.5 %WME | 0.45% @ 12.0 %WME | |
| | | |
| **Estimated sample compression at 6.8 psi** | | |
| 1.24% @ 7.5 %WME | 0.78% @ 7.3 %WME | |
| | | 1.39% @10.9 %WME |
| 2.12% @ 12.5 %WME | 0.91% @ 12.0 %WME | |

## Dynamic Testing

The samples from the first set were subjected to a dynamic transport simulation cycle immediately after they were placed under nominal load, and then once per week for a period of 27 weeks (relatively little change was observed in the first set after 19 weeks). Following dynamic testing of the first set, a second set of dynamic samples was subjected to 47 weeks of testing. Sample heights were measured before and after each cycle of dynamic excitation. Heights of the control samples, which experienced a static load only, were measured weekly as well. The relative change in height for each of these samples is shown in Figure 8. The 6 and 10 %WME samples were loaded to 3.4 psi, while the other samples were loaded to 2.7 psi.

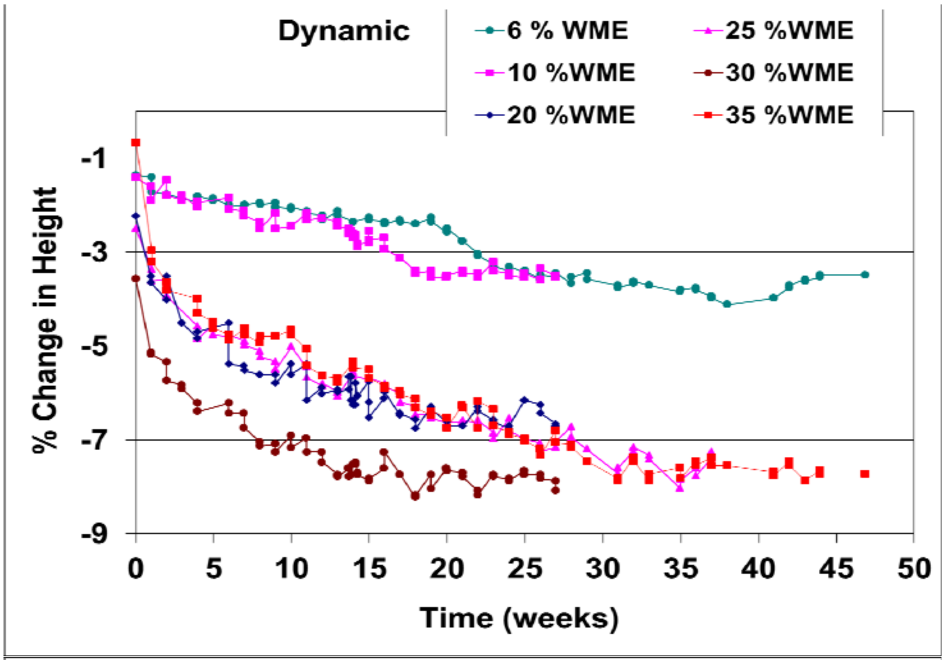


Figure 8A. Relative change in height (strain) under load for dynamic test samples.

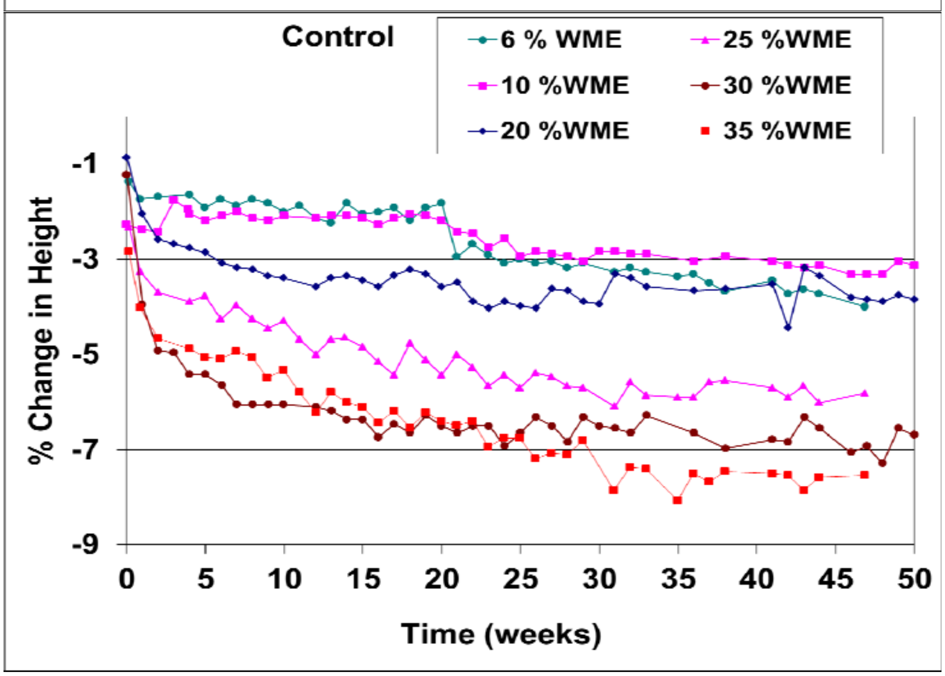


Figure 8B. Relative change in height (strain) under load for static (control) test samples.

**Dynamic Measurements**

During the transport simulation cycle, acceleration measurements were recorded in 2 second intervals for conversion to spectral data in a frequency range of 0-200 Hertz. The dynamic data were captured using a Fast Fourier Transform (FFT) analyzer, in continuous capture mode, to collect all data while the cart was rolled over the rough surface. The FFT analyzer was configured with measurement parameters that included Peak Continuous capture mode (i.e., the peak value measured at each frequency is retained and updated for each increment of the overall measurement), and Hanning Window data smoothing to improve measurement accuracy by minimizing FFT leakage resulting from waveform time-to-frequency domain transformation.

Typical cart dynamic acceleration measurements are shown in Figures 9A through 9D**.** The acceleration response is measured in units of gravity (g), 1 g = ~32 ft/sec$^2$. The measurements in Figures 9A-9B were collected at the beginning of the test program for the first set of samples. The measurements in Figures 9C-9D were collected in the middle of the test program for the second set of samples. "Inst Time" in Figures 9A and 9C is a 2 second interval of the recorded acceleration response for the accelerometer locations. The "Power Spectrum" plots in the Figures 9B and 9D show the acceleration maximum measured for each frequency in the 0-200 Hertz range.

The "Avg=#" in each spectrum plot indicates the number of two second intervals collected to obtain the displayed data. Comparison of Figure 9A with 9C is not performed, because of the transient nature of the time data. However, comparison of the spectral data in Figures 9B and 9D should, and does, show close correlation based on elimination of most transient aspects of the data by conversion to the frequency domain and averaging. Examination of the power spectra, recorded at the two different times in the test program, shows minimal variation over the 9 month duration of testing. Spectra from both dates have approximately the same spectral shape, and a similar broadband input magnitude of ~0.1-0.2 g at the cart floor and on the top of the plastic enclosure.

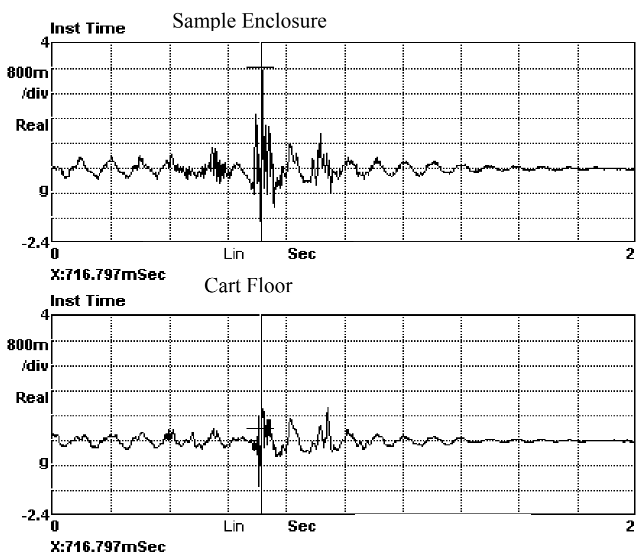


Figure 9A. Two second interval of acceleration response (6/16/10)

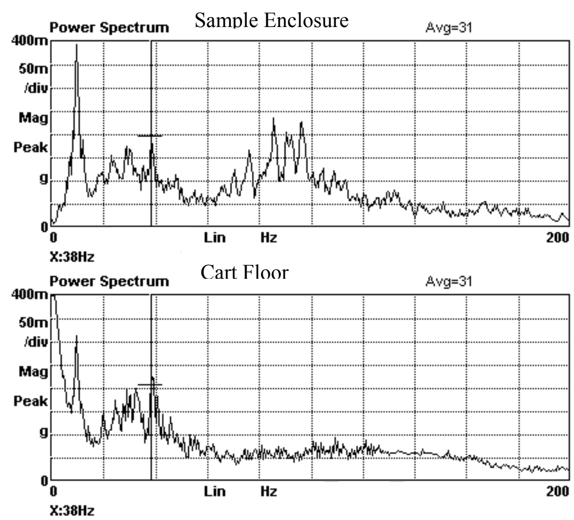


Figure 9B. Spectral Acceleration maxima measured for 31 two second intervals (6/16/10)

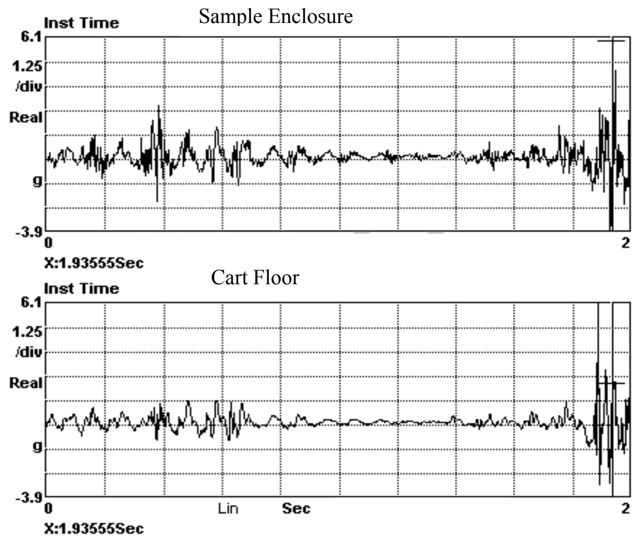

Figure 9C. Two second interval of acceleration response (4/13/11).

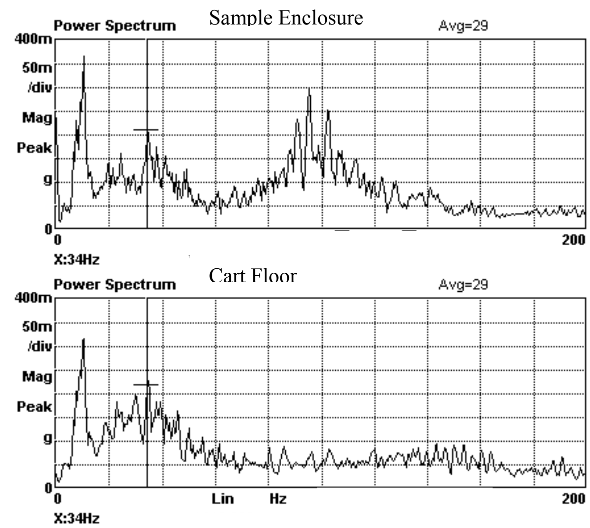

Figure 9D. Spectral Acceleration maxima measured for 29 two second intervals. (4/13/11)

Figure 9E contains an overlay of the background acceleration power spectrum measurements from the 6/16/2010 and 4/13/2011 test dates. For each background measurement, the cart was stationary, and the only input to the cart was due to vibration transmission from the building floor into the cart's wheels. Based on the ~0.003 g peak value, it is obvious that the background acceleration level is insignificant when compared to the Figure 9B 0.1-0.2 g magnitude.

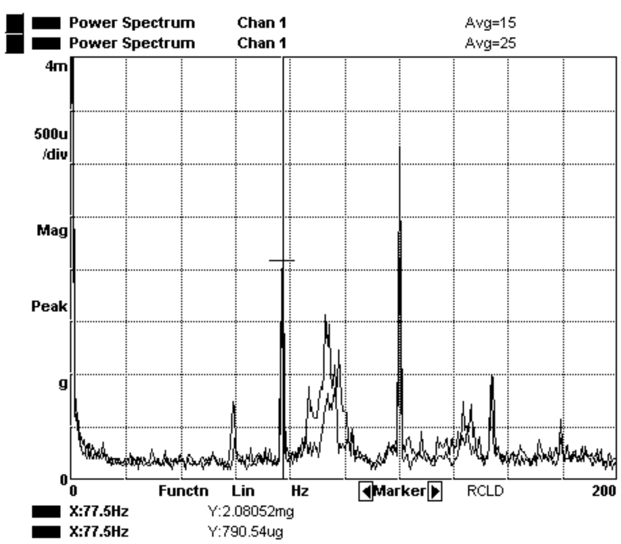

Figure 9E. Floor Input Acceleration data for tests on 6/16/2010 and 4/13/2011

**Damping Testing**

For the first set of experiments, new fiberboard samples were moistened to levels of approximately 10, 20, 30, 40, and 50 %WME. The samples were then subjected to various compressive loads while acquiring Transfer Function (TF) data. The TF data were then processed to obtain the damping for each combination of moisture and compressive load. Full details of the technical aspects of damping data acquisition and damping data reduction are documented separately [12]. The results obtained from the tests are summarized in Table 3, with the damping (%) rounded to the nearest 0.5% increment to review trends. Tabulating damping to increments of 0.1% was deemed to not reflect regular environmental damping variations, and 0.5% was considered to be more indicative of damping variability.

Table 3: New Fiberboard Sample Data Damping for Different Moisture and Compressive Loads

| Test | Weight (lb) | %WME | freq. (hz) | $\zeta$ rounded to 0.5% |
|---|---|---|---|---|
| H10m10w | 9.9 | 10 | 48.50 | 8.0 |
| H10m20w | 22.1 | 10 | 43.00 | 6.0 |
| H10m30w | 32.0 | 10 | 37.75 | 5.0 |
| H10m40w | 39.2 | 10 | 36.00 | 6.0 |
| H10m50w | 50.3 | 10 | 35.50 | 4.5 |
| H20m10w | 9.9 | 20 | 50.50 | 8.5 |
| H20m20w | 22.1 | 20 | 45.50 | 7.0 |
| H20m30w | 32.0 | 20 | 39.25 | 6.5 |
| H20m40w | 39.2 | 20 | 36.25 | 7.0 |
| H20m50w | 50.3 | 20 | 34.00 | 6.0 |
| H30m10w | 9.9 | 30 | 44.00 | 9.5 |
| H30m20w | 22.1 | 30 | 37.25 | 7.5 |
| H30m30w | 32.0 | 30 | 33.50 | 7.0 |
| H30m40w | 39.2 | 30 | 32.00 | 7.5 |
| H30m50w | 50.3 | 30 | 30.25 | 7.0 |

The data provided in Table 4 were obtained for 3 samples that had been previously aged with moisture, static compressive loading, and dynamic excitation while under compressive load.

Table 4: Aged Fiberboard Sample Data Damping

| Test | Weight (lb) | %WME | freq. (hz) | $\zeta$ rounded to 0.5% |
|---|---|---|---|---|
| D50m06w10 | 9.9 | 6 | 45.00 | 8.50 |
| D50m06w30 | 32.0 | 6 | 36.25 | 5.50 |
| D50m06w50 | 49.2 | 6 | 33.25 | 5.50 |
| D40m25w10 | 9.9 | 25 | 45.00 | 7.50 |
| D40m25w30 | 32.0 | 25 | 37.00 | 5.50 |
| D40m25w50 | 49.2 | 25 | 33.50 | 5.50 |
| D40m35w10 | 9.9 | 35 | 44.00 | 8.50 |
| D40m35w30 | 32.0 | 35 | 34.00 | 6.50 |
| D40m35w50 | 49.2 | 35 | 30.75 | 6.50 |

The aged sample data gives some indication of time dependent behavior when compared to the damping results obtained for new fiberboard samples. The data presented in Table 5 were obtained for two new samples, where one was kept at ~10 %WME, and the other ~20 %WME. Both samples were initially tested to obtain damping with a 40 pound compressive load. They were then placed under a static 40 pound load, and tested weekly to obtain the damping value. The goal of this test was to determine how fiberboard damping changed with time due to the effects of the continuous static compressive loading.

Table 5: New Fiberboard Sample Time Dependent Damping (40 pound compressive load)

| File | 2012 Test Date | %WME | freq. (hz) | ζ rounded to 0.5% |
|---|---|---|---|---|
| 10H020212 | 2-Feb | 10 | 34.00 | 4.5 |
| 10H020912 | 9-Feb | 10 | 33.25 | 4.0 |
| 10H021512 | 15-Feb | 10 | 35.50 | 4.0 |
| 10H022212 | 22-Feb | 10 | 34.25 | 4.5 |
| 10H022212b | 22-Feb | 10 | 34.50 | 4.0 |
| 10H022912 | 29-Feb | 10 | 35.25 | 4.5 |
| 10H031412 | 14-Mar | 10 | 34.25 | 4.5 |
| 20H020212 | 2-Feb | 20 | 34.50 | 5.0 |
| 20H020912 | 9-Feb | 20 | 37.00 | 3.5 |
| 20H020912b | 9-Feb | 20 | 37.25 | 4.0 |
| 20H021512 | 15-Feb | 20 | 38.00 | 3.5 |
| 20H022212 | 22-Feb | 20 | 37.75 | 4.0 |
| 20H022212b | 22-Feb | 20 | 38.75 | 4.0 |
| 20H022912 | 29-Feb | 20 | 36.75 | 4.0 |
| 20H031412 | 14-Mar | 20 | 36.00 | 4.0 |
| 20H032112 | 20-Mar | 20 | 36.75 | 4.0 |

## DISCUSSION

### Short-Term Testing

In the short-term tests (see Figure 6), the initial loading cycle (2.7 or 3.4 psi) is indicative of the response of the lower layers of the fiberboard assembly when the package is first assembled. Similarly, the second loading cycle (5.4 or 6.8 psi) might approximate the response during some period of handling or transport. The removal of the higher load represents an end to the dynamic activity as the package sits in storage. For samples tested under a nominal stress of 2.7 psi (from both stages of testing) some scatter is seen, but the overall trend is that compaction increases approximately linearly with moisture content, up to the saturation point (28 wt% moisture, or approximately 38 %WME) Above saturation, there is not a significant variation in compaction with increasing moisture content. For the lower moisture levels where samples were tested at both 2.7 and 3.4 psi stress levels, the higher stresses produced higher compaction, as would be expected.

## Compression Testing

Package to package variation is seen in compression test data and in other fiberboard properties [6, 8]. Similar variation would be expected in the response to dynamic loading. The degree of compression predicted by the compression test data for a given stress is less than that measured in the dynamic and short-term samples. Therefore, the compression test data are non-conservative relative to that obtained in dynamic and short-term testing. Accordingly, compression test data should not be used to predict long-term fiberboard compaction.

## Dynamic Testing

Under conditions typical of many packages (~10 %WME, 3.4 psi stress) both the short-term and the initial (up to 5 weeks) dynamic samples show about 2 % strain (reduction in height/original height). Under a static stress of 6.8 psi (essentially a single cycle 1 g load input), the short-term sample experienced additional strain of ~2%. Under dynamic loading, the strain also increased an additional 2 % over the following 15 weeks. Although both sets of samples reached approximately the same final strain, the dynamic samples approached this value much more slowly because of the lower magnitude of dynamic loading (~0.1 g for the dynamic sample, ~1 g for the short-term sample). In comparison to these results, the compression test sample experienced less strain at 3.4 psi (~0.7%) and at 6.8 psi (1.4%). This likely results from the immediate measurement of sample displacement during the compression test rather than allowing the sample to settle for a short period before measuring the height.

In the dynamic samples, the degree of compression observed in the second set of samples is not entirely consistent with that for the first set. Each sample of the second set took longer to reach an equilibrium height than the samples in the first set. The final degree of compaction is about the same for the 25, 30 and 35 %WME dynamic samples, although not for the static samples (see Figure 8). The accelerometer data shows the dynamic input is essentially the same for both sample sets. The reason for these behaviors is not fully understood, but might be attributable to the following causes:

- Variation in fiberboard properties from different regions within the package. Such variation has been seen in other testing.
- Variation in ambient temperature throughout the test. The two sets began testing at different times of the year, and the lab experiences seasonal temperature cycles.
- Other parametric differences not yet identified.

During the 7$^{th}$ week dynamic cycle for all samples in the first sample set, the dynamic cycle was extended to 10 times the duration. However, the degree of compression experienced by each of the samples was not significantly different from that experienced in the other dynamic cycles. It is postulated that the fiberboard is limited in the degree to which it can compact within a relatively short period, and that additional dynamic input will not create significant additional compaction.

**Dynamic Measurements**

The safety analysis for the 9975 package includes discussion of the vibration from road transportation loadings [11]. The vibration levels are bounded by a high amplitude low frequency envelope of 1 – 1.5 g at 2 – 7 Hz, and a power spectral density value of 0.001 $g^2$/Hz in the frequency range from 10-40 Hz. The low frequency high acceleration input would not result in significant packaging response due to the higher resonant frequencies indicated in packaging qualification calculations. However, input over the 10-40 Hz range would result in significant package response, as this is where the fundamental frequency of the system occurs, and as such defines the input envelope and a conservative bound to typical vibrations experienced on a smooth road. Similar loadings might be postulated to result from handling packages within a facility.

The measured displacement data for the first sample set (Sample IDs 50C, 40E, 40F), and the second sample set (Sample IDs D-50-6, D-40-25, D-40-35) are included in Table 6.

Table 6. Measured Response Data

| Sample ID | Nominal Moisture Content %WME | [A] Initial Sample Height w/o weight (in) | [B] Initial Height with weight (in) | [W] Weight Added (lb) | [D] Final Height with Weight (in) | [E] Final Height w/o Weight (in) |
|---|---|---|---|---|---|---|
| 50C | 10 | 2.116 | 2.095 | 50.6 | 2.041 | 2.07 |
| 40E | 20 | 2.192 | 2.166 | 40.7 | 2.045 | 2.069 |
| 40F | 30 | 2.300 | 2.262 | 40.5 | 2.114 | 2.139 |
| D-50-6 | 6 | 2.208 | 2.191 | 50.6 | 2.032 | 2.165 |
| D-40-25 | 25 | 2.292 | 2.270 | 40.7 | 2.118 | 2.153 |
| D-40-35 | 35 | 2.278 | 2.252 | 40.5 | 2.078 | 2.099 |

In the context of this study, important sample dynamic parameters include stiffness, damping, and natural frequency. The Transport Acceleration Response (TAR), defined here as the vibration input level design requirement associated with the specific mode of transport, is a function of these sample dynamic parameters. The TAR value is used for comparison to test input to assess how well the tests simulate package road induced response. Using the data in Table 6, it is possible to calculate stiffness, natural frequency, and TAR for each individual sample. Results for the sample dynamic parameters, obtained using the Table 6 data and the same dynamic analysis methodology implemented for 9975 package qualification, are provided in Table 7. The dynamic system model used for the 9975 closely matches the loaded sample configuration used for these tests where a rigid mass is provided vertical support by fiberboard.

The stiffness of the container inside the 9975 is considered sufficiently high to decouple rigid body response of the content/fiberboard system from the flexible response of the container. For this package system, the fundamental resonant frequency was calculated as ~22 Hz in the 9975 evaluation. The TAR, corresponding to this frequency and a damping value of 10% was determined to be 0.42 g. In comparison to the dynamic testing acceleration input shown in Figures 9B and 9D, the 0.1-0.2 g input is 25-50% of the TAR requirement with an assumed fiberboard damping value of 10%. The cumulative duration of dynamic excitation for sample set 1 was approximately 1 hour over 6 months. There is not a TAR exposure duration design requirement available that can be compared to the duration of dynamic testing. The approximate

1 hour of sample dynamic input included continuous shock input, which is analogous to subjecting a package to one hour of continuous travel on a very rough or hole riddled road. The shock input, typical during testing, is indicated by the high amplitude short duration acceleration values in Figures 9A and 9C.

In regard to fiberboard damping, the exact value of damping was not initially determined experimentally. Since a damping value of 10% was used in the packaging design calculations, 10% is also used here, for all samples regardless of moisture content, to calculate the TAR.

The sample dynamic parameter results listed in Table 7 were obtained using the following equations:

$f=(386.4K/W)^{1/2}/2\pi$, [Ref 11, pages Appendix 2.2, pages 87-90]
K=Sample Stiffness (lb/in)
W=Compression Weight (lb)
f=fundamental resonant frequency (Hz)

$G_{out}=(\pi PfQ/2)^{1/2}$, [Ref 11, Appendix 2.4 pages 54-56]
P=0.001 $g^2$/Hz, transportation power spectral density for $10 \leq f \leq 40$ Hz
$G_{out}$=Transport Acceleration Response (g)
Q=Amplification factor=$1/(2\zeta)$
$\zeta$ =Damping ratio, 10%

Examination of the Table 7 data results in several noteworthy observations. Although natural frequency is a function of stiffness, the natural frequency results do not vary as much as the stiffness. The calculated range of natural frequency values (16-24 Hz) is in good agreement with the package documented value of 22 Hz from the SARP [11]. All samples experienced permanent compression (Column [F]) with values increasing proportional to the moisture level. For the 30 %WME sample, the initial compression caused by weight addition was not recovered when the weight was removed, as indicated by comparison of the initial sample compression (Column [C]) and the sample elastic rebound (Column [G]). This is indicative of an overall change in sample stiffness during the dynamic test period. The other samples from set 1 fully recovered initial compression despite experiencing some permanent compression. All tests show changes in total sample compression (Column [H]), sample compression after the weight was added (Column [I]), and permanent deformation that occurred during the dynamic test sequence (Column [J]) respectively. The data for each of these quantities show a trend of increasing value with an increase in moisture level.

The stiffness and fundamental resonant frequency are calculated for both sets of dynamic samples in Table 7. Note that both of these parameters tend to decrease as the moisture level increases. The two exceptions to this trend are seen with the 25 and 35 %WME samples in the second set. In both of these samples, each parameter has a higher value than would be expected based on the trend displayed by the other samples. It is noted that these two samples also deviated from the overall trend in the amount of compression. A cause of this deviation has not yet been identified, but it is noted that fiberboard is inherently heterogeneous, and variation in properties should be expected.

Table 7: Calculated Dynamic Response Data

| Sample ID | Nominal Moisture Content %WME | [C]=A-B Initial Sample Compression (in) | [F]=A-E Permanent Compression (in) | [G]=E-D Sample Elastic Rebound (in) | [H]=A-D Total Compression with Weight (in) | [I]=B-D] Sample Deformation Post Weight Addition (in) | [J]=B-E Permanent Deformation after initial compression (in) | [K]=W/C Stiffness K (lb/in) | Fundamental Resonant Frequency f (Hz) | Transport Acceleration Response TAR (g) |
|---|---|---|---|---|---|---|---|---|---|---|
| 50C | 10 | 0.021 | 0.046 | 0.029 | 0.075 | 0.054 | 0.025 | 2410 | 21.59 | 0.41 |
| 40E | 20 | 0.026 | 0.123 | 0.024 | 0.147 | 0.121 | 0.097 | 1565 | 19.40 | 0.39 |
| 40F | 30 | 0.038 | 0.161 | 0.025 | 0.186 | 0.148 | 0.123 | 1066 | 16.05 | 0.36 |
| D-50-6 | 6 | 0.017 | 0.043 | 0.133 | 0.176 | 0.159 | 0.026 | 2976 | 23.99 | 0.43 |
| D-40-25 | 25 | 0.022 | 0.139 | 0.035 | 0.174 | 0.152 | 0.117 | 1850 | 21.09 | 0.41 |
| D-40-35 | 35 | 0.026 | 0.179 | 0.021 | 0.200 | 0.174 | 0.153 | 1558 | 19.40 | 0.39 |

The effects of the dimensional changes on package dynamics can be postulated based on the Table 7 results. Since the overall height of the fiberboard samples decreased, the fiberboard experienced "sag" due to either slow creep under the constant static load, or slow creep with possible additional sag contribution from the dynamic excitation. It is likely that the overall shock absorption capability of the reduced fiberboard column also decreased. However, the initial shock absorption capability of the fiberboard was excessive in regard to demand, and the reduction due to sagging of the fiberboard is likely small.

For samples 40E and 50C, the initial deformation due to weight addition is approximately equal to the sample rebound. This result indicates that the sample stiffness was unchanged at the end of the 6 month test period. In contrast, sample 40F did not recover a substantial amount of the initial compression. This indicates that the overall stiffness of 40F has increased to approximately that of 40E, based on nearly identical rebound values in column [G]. Since the variation in stiffness and natural frequency for all of the samples only results in a difference of ~0.05 g for the TAR, the change in fiberboard stiffness would have a minimal effect on the dynamic behavior of the 9975 package/container system. However, given a substantial increase in the fiberboard stiffness, due to greater sagging, it is possible that natural frequency increases coupled with a reduction in damping could result in higher loads experienced by package contents. Once again, the margin between capacity and demand related to vibration loading is great, and a limited amount of sagging should not produce unacceptable response. Based on the test data presented, a 5% reduction in sample 40F height was measured, and limiting package post loading deformation to a similar value would likely provide a conservative bound for maintaining acceptable package dynamic response.

Examination of Figures 9A through 9D shows higher acceleration values in both "Inst Time" and "Power Spectrum" plots for the accelerometer mounted on the sample enclosure. This result is expected as the hard steel and plastic enclosure has additional flexibility which amplifies the base input. Since multiple sample enclosures are placed on the cart for dynamic loading, the dynamic acceleration imparted to each sample from the cart floor would be slightly different, but bounded by the "Sample Enclosure" and "Cart Floor" data.

The power spectrum for "Cart Floor" in Figure 9D is considered typical for sample dynamic loading. The spectrum indicates a fairly uniform acceleration input of 0.1-0.2 g in the 5-200

Hertz frequency range. Excitation in the 0-5 Hertz range is low, as expected, due to the hardness of the cart wheels, and steel expanded metal surface. The hard surfaces of contact result in a broad frequency range of input, as opposed to a smaller range of low frequency input if the duration of impact were increased by using softer material for the cart wheels. Since the mass mounted on the top of each sample is rigid, the dynamic force experienced by a sample would be equivalent to the input acceleration multiplied by the weight of the compressing object, applied as a sinusoidal load over duration equal to time spent rolling the cart over the rough surface. Additionally, the peak static equivalent dynamic shock load can be approximated by multiplication of the compressive weight by the peak acceleration value shown in either Figure 9A (>3 g) or 9C (~6 g). This is a very short duration acceleration, and as such, mechanical response or stress assessment would need to take into account time dependent properties for shock effect evaluation.

**Damping Testing**

Figure 10 includes the data from Table 3 plotted for the purpose of viewing damping changes as a function of moisture level for a given compressive load. From Figure 10, the variation in moisture for a given compressive load results in a range of 1.5-2.5 percentage points in damping level for new fiberboard material. The variation in compressive load from 10-50 pounds results in a 2.5-3.5 percentage point change in damping level.

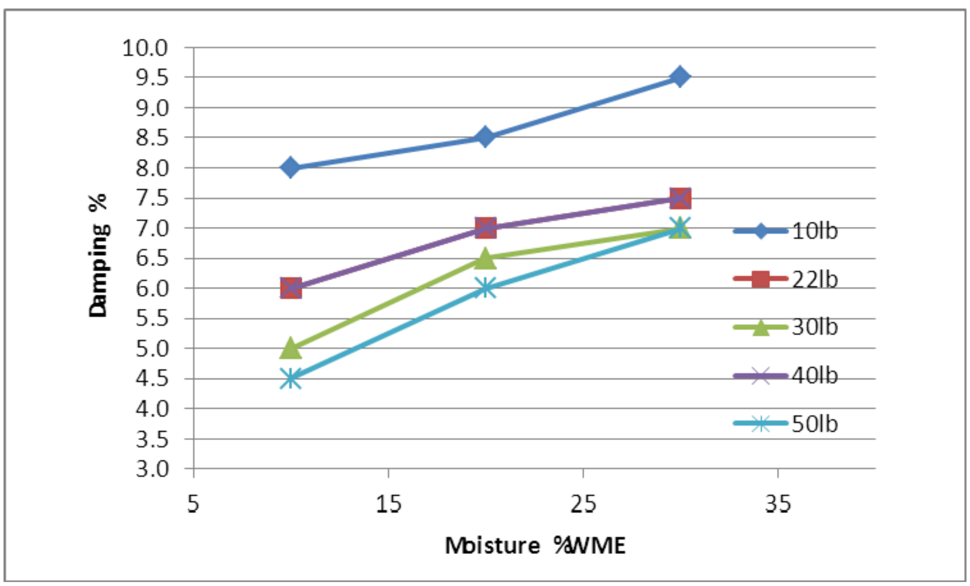


Figure 10. New Sample Damping for various Compressive Loads as a function of Moisture Level

An observation from Figure 10 is that the damping level for the lightest load of 10 pounds is significantly higher than for the heavier loads. This may be attributable to the limited compression of the open cell structure of the fiberboard which acts to damp vibration as the cells are compressed.

Figure 11 includes the data from Table 3 plotted to view damping changes as a function of compressive load at a given moisture level. Figure 11 shows a gradual reduction in damping level as the compressive load increases, except for an increase in damping at a compressive load of 40 pounds for all three moisture levels. No explanation is provided for the damping increase at the 40 pound compressive load. It is possible that measurement error or environmental factors are responsible for the variation, even though it is present for all three moisture levels. Rounding of damping (%) to 0.5%, combined with measurement variability, results in a potential 1% damping range (e.g., tabulated value of 4.5% could be anywhere in range from 4% to 5%). For -0.5% adjustment of the 40 pound damping values, and a +0.5% damping increase for the 30 pound compressive load at 30% moisture, all Figure 11 curves would show an asymptotic reduction for all damping values as compressive load increases.

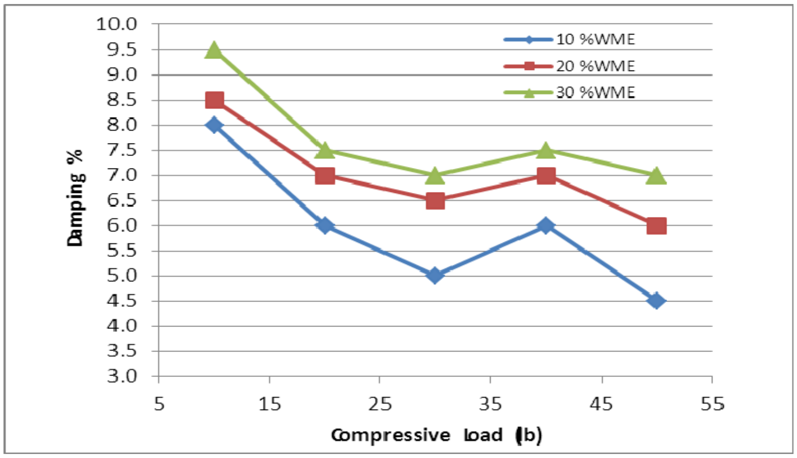


Figure 11. New Sample Damping for various Moisture levels as a function of Compressive Load.

Figure 12 shows the Table 4 damping data plotted as a function of compressive load for each aged sample. All three samples show similar behavior where additional change in the damping value does not occur once a sufficiently large compressive load is applied.

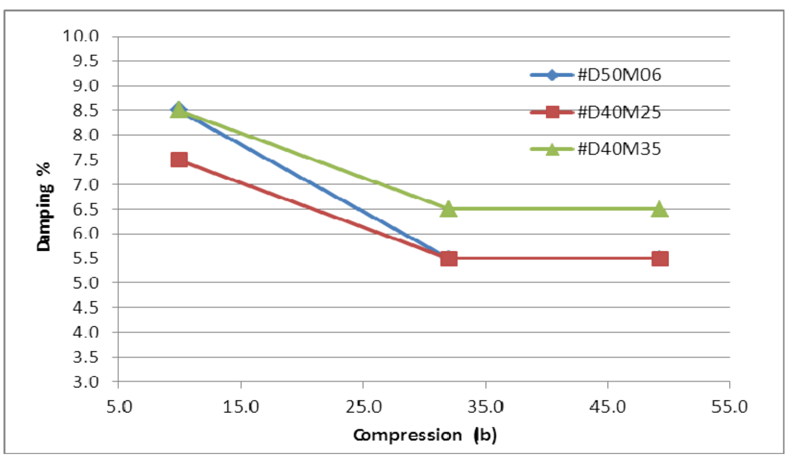


Figure 12. Aged Fiberboard Sample Damping for Different Compressive Loads

This behavior is similar to the test data for the new samples, except that the compressive load at fixed damping is slightly lower, where the range is 7.0%-9.0% for the aged samples and 7.5%-10% for the new samples, when the 0.5% variability is taken into account. This result is likely attributable to aging of the samples. Exposure to high compressive loading (40 or 50 pounds), and dynamic loading have resulted in a loss of some open cell structure due to creep or slumping of the moist fiberboard over time. The aged samples exhibit an overall lower damping, and a lower load threshold where the sample loses any damping contribution from further increases in compressive loading.

The data curves in Figure 13 show that during the initial period of static compression, the damping has some variability. However, the variability is small, and after only a few weeks of exposure, the samples exhibited a constant damping value (3.5% to 5% range accounting for 0.5% variability) similar to what was obtained for the aged sample data in Figure 12 with 30 pound compressive loading (5%-7% range accounting for 0.5% variability). While the 10 %WME and 20 %WME damping values are only separated by 0.5% in Figure 13, it was expected that the 10% value would have a higher damping value due to reduced slumping or creep in response to the static loading (i.e., higher moisture level in fiberboard would result in greater permanent compression).

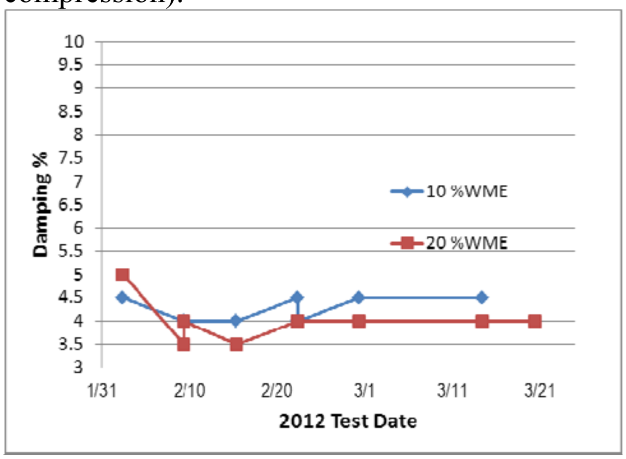


Figure 13. New Fiberboard Sample Time Dependent Damping for 40 pound Compressive Load

**General Discussion**

At elevated moisture levels (≥ 20 %WME), the compaction strain is higher with the increased moisture level, and strain continues to increase for a longer period of time. This behavior is seen in all samples - dynamic, control (static), and short-term. However, the rate of compression of the dynamic sample while between dynamic cycles is less than the rate of compression of the control (static) sample. As each of the short-term samples is unloaded, there is some recovery of sample height, but some compression remains.

In general, higher fiberboard moisture content corresponds to higher total compaction, a greater rate of compaction, and continued compaction over a longer period of time. An additional trend was observed in the dynamic testing - as moisture levels fluctuate, the sample height tends to fluctuate in unison. This correlation with moisture fluctuation was stronger for moisture levels from 20 %WME to 30 %WME as illustrated in Figure 14. This additional trend would be expected for the short-term samples, but was not verified during the tests.

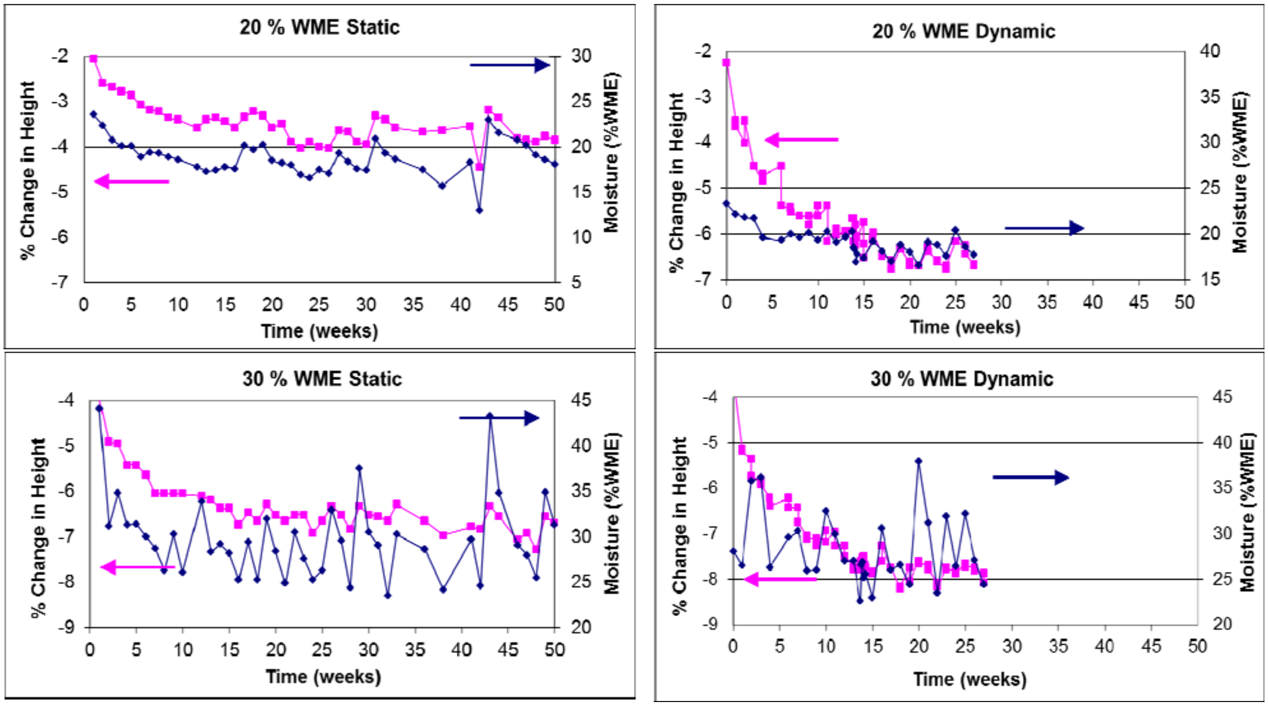


Figure 14. Typical correlation between moisture content and compression behavior, shown for 20 and 30 %WME static (control) and dynamic samples.

Figure 15 shows the final compaction data from the short-term and dynamic compaction tests, combined into a single presentation. Relatively little difference in compaction is seen between the short-term, dynamic and static (dynamic control) samples. The trendline shown in Figure 15 shows the behavior with all of the samples tested at 2.7 psi averaged together. This behavior is linear up to the saturation point, and appears to have little variation with moisture level above saturation.

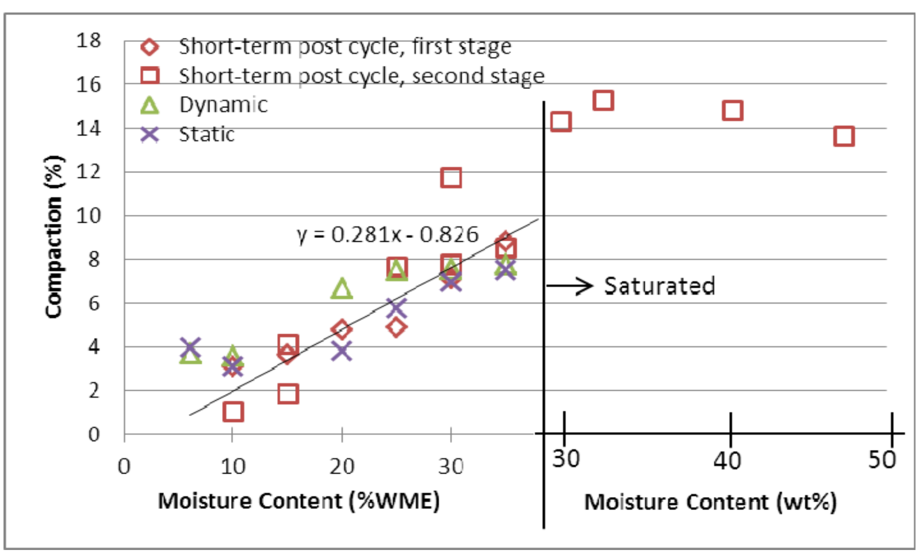


Figure 15. Final compaction data from short-term and dynamic compaction tests. The trendline is a linear fit to all data below the saturation point (~38 %WME) and a stress of 2.7 psi.

With an internal heat load in the 9975 packages, several changes are expected to occur. The heat load will create a thermal gradient through the fiberboard, and the fiberboard moisture will redistribute preferentially to the cooler regions of the package. For typical package heat loads and service environments, the degree of moisture redistribution is modest. However, for maximum heat loads and high external temperatures (especially as the local fiberboard temperature approaches the boiling point of water), a significant amount of moisture can redistribute to the bottom of the package, up to and beyond the point of fiberboard saturation (~38%WME or 28 wt %).

As the moisture content of the bottom layers increases, the compressive strength of those layers will decrease and the layers will compact, as seen in this testing. This observed compaction is a net effect of two competing phenomena – the weakened fiberboard compacts under the load of the internal components, and the fiberboard fibers swell from the absorption of additional water. This net compaction of the bottom layers will directly add to the axial gap. At the same time, the middle region of the fiberboard assembly (which is typically the hottest) has lost moisture, and will shrink axially. The upper fiberboard assembly initially rests on the lower fiberboard assembly, with a nominal 0.25 inch gap between the shield lid and the upper assembly bearing plate. (With combination of tolerances, this gap can be as low as 0.05 inch.) As the middle fiberboard region shrinks axially, this will also contribute directly to the axial gap at the top of the package, until the upper assembly is resting on the shield lid. After that, additional shrinkage will open a gap between the upper and lower fiberboard assemblies. Therefore, shrinkage of the middle fiberboard region can contribute at least 0.05 inch, and up to 0.25 inch for the nominal case, to the axial gap. Additional shrinkage of the middle fiberboard region will not contribute to further increases in the axial gap.

At least some of the fiberboard above the bearing plate in the upper assembly is also at elevated temperature, and moisture redistribution from this area will also occur. The presence of the air shield (stainless steel cover partially surrounding the upper fiberboard assembly) could reduce the rate of moisture loss, but should not prevent it. Therefore it will be conservative to ignore any contribution of this area to the axial gap. The current process of measuring the 1" maximum gap provides criterion screening tool for identifying significant fiberboard degradation within 9975 packages. Packages identified with an axial gap exceeding this criterion will be removed from service for further examination. An analysis of the Figure 15 data indicates that the axial gap will increase by 0.282 inch as the moisture content of the bottom fiberboard layers approaches saturation, and will increase by 0.405 inch above saturation. Combining this result with the observed variation in axial gap of packages in storage (assuming otherwise nominal dimensions of package components) predicts that 92% of packages reaching saturation of the bottom fiberboard layers will exceed the axial gap criterion. [13]

The data described in this report were generated from lab scale samples, but full size packages are expected to show these same trends. These trends are consistent with observations from packages removed from service in which fiberboard with elevated moisture levels became compacted, leading to an increased axial gap. This data was specifically measured on cane fiberboard. It is expected that softwood fiberboard will exhibit similar trends, since the two materials have shown similar behavior in other properties. However, it should not be assumed that the two materials will behave identically.

## CONCLUSIONS

Moisture levels and dynamic loading contribute to the compaction of the fiberboard. For a given moisture level, dynamic loadings on the fiberboard will lead to greater compaction than static loading. Beyond a certain degree of compaction, continued dynamic loading causes little additional compaction. Rather, subsequent change in fiberboard height is driven more by variation in moisture content.

The exposure of the samples to dynamic excitation indicates a general trend of greater compaction for higher moisture levels. There appears to be a threshold moisture level where fiberboard initial compression becomes unrecoverable. Below this threshold, the fiberboard would show no change in dynamic response, but may have slightly reduced shock absorption capabilities. Negative transportation effects due to fiberboard "sag" may be avoided by in-service inspection of the fiberboard height reduction with time. The current practice of verifying that the axial gap at the top of the package is less than 1 inch provides confidence against excessive reduction of fiberboard height. Above the threshold moisture value, the fiberboard stiffness increases, but based on an increase in the fundamental resonant frequency, the net effect may result in either slightly higher or even significantly lower transportation dynamic loading depending on the final stiffness. The shock absorption capability of the higher moisture exposure would result in reduced shock absorption capability based on higher fiberboard stiffness, and the related reduced fiberboard height.

Based on the damping test results, the following conclusions are presented:

1. For a fixed moisture level, fiberboard material damping is higher at light loading due to greater open cell structure resistance to vibration.
2. Higher moisture levels result in higher damping levels for light loading.
3. Increased compressive loading results in damping value convergence for variations in %WME.
4. Aging of the fiberboard with adequate levels of moisture and compressive loading, results in creep or slumping of the material such that damping decreases to a value independent of compressive loading.
5. Analytical representation of the fiberboard would require knowledge of the history of combined moisture and compressive loading exposure. However, stiffness and damping may be conservatively approximated by using 4% damping along with stiffness/mass values consistent with a 33hz damped natural frequency obtained for a 4"x4"x2.2" sample compressed with a 40 pound load.

**References**

[1] SRNS-TR-2010-00044, "Task Technical and Quality Assurance Plan for Testing of Moisture Effects on Model 9975 Package (U)", T.M. Stefek, W. L. Daugherty, March 2010.

[2] WSRC-TR-2001-00286, "SRS Surveillance Program for Storage of Pu Material in KAMS", Rev 4, July 2008.

[3] SRNL-STI-2009-00742, "Examination of Shipping Packages 9975-01818, 9975-01903 and 9975-02287 (U)", W. L. Daugherty, November 2009

[4] SRNL-STI-2011-00734, "Examination OF Shipping Packages 9975-02274 and 9975-04769 (U)", W. L. Daugherty, December 2011

[5] PVP2010-25087, "Effects of Moisture in the 9975 Shipping Package Fiberboard Assembly", W. L. Daugherty. K. A. Dunn, J. L. Murphy and E. R. Hackney, Proceedings of PVP2010, ASME Pressure Vessels & Piping Division Conference, July 18-22, 2010, Bellevue, WA.

[6] PVP2010-25118, "Aging Model for Cane Fiberboard Overpack in the 9975 Shipping Package", W. L. Daugherty and S. P. Harris Jr, Proceedings of PVP2010, ASME Pressure Vessels & Piping Division Conference, July 18-22, 2010, Bellevue, WA.

[7] PVP2007-26114, "Properties of Fiberboard Overpack Material in the 9975 Shipping Package Following Thermal Aging", W. L. Daugherty, Proceedings of PVP2007, ASME Pressure Vessels & Piping Division Conference, July 22-26, 2007, San Antonio, TX.

[8] "Compaction of Fiberboard Overpack Materials in a 9975 Shipping Package" T. M. Stefek, W. L. Daugherty, E. G. Estochen, J. L. Murphy, Proceedings of INMM Institute of Nuclear Materials Management 51st Annual Meeting, July 11–15, 2010, Baltimore, MD.

[9] Research Note FPL-RN-0268, "Equilibrium Moisture Content of Wood in Outdoor Locations in the United States and Worldwide", W. T. Simpson, Forest Products Laboratory, Forest Service, U.S Department of Agriculture, Madison WI, 1998

[10] PVP2005-71568, "Mechanical Properties of Fiberboard Overpack Materials in the 9975 Shipping Package", W. L. Daugherty and P. R. Vormelker, Proceedings of PVP2005, ASME Pressure Vessels & Piping Division Conference, July 17-21, 2005, Denver, CO

[11] S-SARP-G-00003, "Safety Analysis Report for Packaging Model 9975", Revision 0, Appendix 2.2, January 2008.

[12] SRNL-L4420-2012-00006, "Fiberboard Damping Measurements", E. G. Estochen, 6/6/2012.

[13] SRNL-STI-2012-00429, "Analysis of the Axial Gap vs Fiberboard Moisture Content in a 9975 Shipping Package", W. L. Daugherty, March 2013

CC: J. S. Bellamy, 773-41A
G. T. Chandler, 773-A
W. L. Daugherty, 773-A
K. A. Dunn, 773-41A
E. G. Estochen, 773-A
T. W. Griffin, 705-K
T. J. Grim, 105-K
E. R. Hackney, 705-K
N. C. Iyer, 773-41A
D. R. Leduc, 773-41A
J. W. McEvoy, 707-42B
L. C. Olson, 773-A
T. M. Stefek, 773-41A
K. E. Zeigler, 773-41A
Document Control